Morphology and Mechanical Properties of Layered Silicate Reinforced Natural and Polyurethane Rubber Blends Produced by Latex Compounding

S. Varghese,[1] K. G. Gatos,[2] A. A. Apostolov,[3] J. Karger-Kocsis[2]

[1]*Rubber Research Institute of India, Kottayam, Kerala-686009, India*
[2]*Institut für Verbundwerkstoffe GmbH (Institute for Composite Materials), Kaiserslautern University of Technology, P.O. Box 3049, D-67653 Kaiserslautern, Germany*
[3]*Laboratory on Polymers, University of Sofia, BG-1126, Sofia, Bulgaria*

Received 5 September 2003; accepted 29 October 2003

ABSTRACT: Natural rubber (NR), polyurethane rubber (PUR), and NR/PUR-based nanocomposites were produced from the related latices by adding a pristine synthetic layered silicate (LS; sodium fluorohectorite) in 10 parts per hundred parts rubber (phr). The dispersion of the LS latices in the composite was studied by X-ray diffraction (XRD) and transmission electron microscopy (TEM). Further information on the rubber/LS interaction was received from Fourier transform infrared spectroscopy (FTIR) and dynamic mechanical thermal analysis (DMTA). Tensile and tear tests were used to characterize the performance of the rubber nanocomposites. It was found that LS is more compatible and thus better intercalated by PUR than by NR. Further, LS was preferably located in the PUR phase in the blends, which exhibited excellent mechanical properties despite the incompatibility between NR and PUR. Nano-reinforcement was best reflected in stiffness- and strength-related properties of the rubber composites. © 2004 Wiley Periodicals, Inc. J Appl Polym Sci 92: 543–551, 2004

Key words: clay; latices; nanocomposites; rubber; structure–property relations

INTRODUCTION

Nowadays rubber nanocomposites containing layered silicates (LS) as reinforcement are gaining importance.[1] The interest behind this development is due to the nanoscale dispersion (the thickness of the layered silicates is ca. 1 nm) and the very high aspect ratio of the silicate platelets (length-to-thickness ratio up to 2000),[2] enabling high reinforcing efficiency even at low LS loading. To make the polar LS compatible with nonpolar polymers and thus to facilitate the exfoliation of LS, the silicates are made organophilic (e.g., [2–3]). This occurs by exploiting the cation exchange capacity of the LS. Organophilic LS are, however, expensive, which forced researchers to have a look at alternative methods. Nonorganophilic (pristine) LS can be dispersed in water, which acts as swelling agent via hydration of the intergallery cations (usually Na^+ ions). Note that several rubbers are available in latex form, which is a rather stable aqueous dispersion of fine rubber particles (particle size below 5 μm). Mixing of latex with LS, followed by coagulation, is therefore an interesting way to produce rubber nanocomposites. This route has been already followed for natural (NR),[4] styrene/butadiene (SBR),[5–6] acrylonitrile/butadiene (NBR),[7] and carboxylated NBR.[8] On the other hand, no report is available on LS-reinforced latex blends. This is quite surprising as latex combinations are widely used to improve some praxis-relevant properties of the constituents. Note that NR has to be filled/reinforced owing to its moderate tear strength [e.g., [9–10]]. To improve the resistance to solvents (especially toward hydrocarbons), abrasion, and UV irradiation, NR is often blended with polyurethane rubber (PUR). Accordingly, the aims of this present work were (1) to produce LS-reinforced NR/PUR-based nanocomposites via latex compounding, and (2) to study their morphology-dependent mechanical properties.

EXPERIMENTAL

Materials

As LS, a synthetic sodium fluorohectorite (Somasif ME-100) of Co-Op Chemicals (Tokyo, Japan) was selected. This LS had a cation exchange capacity of 100 meq/100 g and an intergallery distance of 0.95 nm. Note that this LS exhibits a very high aspect ratio (viz. >1000).[4,11]

Correspondence to: J. Karger-Kocsis (karger@ivw.uni-kl.de).
Contract grant sponsor: Alexander von Humbolt Foundation.
Contract grant sponsor: German Science Foundation; contract grant number: DFG-GRK 814.
Contract grant sponsor: German Academic Exchange.

TABLE I
Formulation of NR Prevulcanized Latex

	Formulation	
	Wet	Dry
NR latex (60%)	166.7	100.0
10% KOH solution	1.0	0.1
50% ZDMC dispersion	2.0	1.0
50% sulfur dispersion	2.0	1.0

ZDMC, zincdimethyldithiocarbamate.

Sulfur prevulcanized NR latex, along with the ingredients, were procured from Rubber Research Institute of India (Kottayam, Kerala, India). This concentrated, high-ammonia (1%) NR latex contained 60% dry rubber. For prevulcanization, this latex was mixed with the ingredients listed in Table I under slow stirring. The compounded latex was then heated to 70°C in a water bath with low stirring for 4 h. The prevulcanized latex obtained was cooled to room temperature and the initial ammonia content was restored by adding ammonia solution. The NR latex was then stored in tight plastic bottles until use.

PUR latex (Impranil DLP-R) containing ~ 50% polyester-based polyurethane was supplied by Bayer (Leverkusen, Germany).

Film casting

The prevulcanized NR latex was mixed with the aqueous dispersion of LS (10%) and stirred well. The dirt and coarse particles were removed by filtering through a sieve (with an opening of 250 μm) and the latex compound was cast in a mold built of glass plates (dimensions: 130 × 100 × 2 mm). The casting was allowed to dry in air until transparent and post-vulcanized at 100°C for 30 min in an air-circulated oven. Fully vulcanized samples were then cooled and packed in sealed polyethylene bags for testing.

Aqueous dispersion of LS was added to the PUR latex, stirred, and cast as indicated above and air dried until transparent. Note that the PUR was not cured.

Latex blends with various PUR/NR ratios (viz. 1/1 and 8/2) with and without LS were produced in a similar way as described above.

Morphology detection

The dispersion of LS in the latex films was studied by X-ray diffraction (XRD) and transmission electron microscopy (TEM). XRD spectra were obtained in the transmission mode by using Ni-filtered CuKα radiation (λ = 0.1542 nm) by a D500 diffractometer (Siemens, Munich, Germany). The samples were scanned in the step mode at a 1.5°/min rate in the range of $2\theta < 12°$. For comparison purposes, the XRD spectrum of the LS powder was also registered, however, in reflection.

TEM images were taken with a LEO 912 Omega microscope (Oberkochen, Germany) at an accelerator voltage of 120 kV. Thin sections (ca. 100 nm) of the specimens were cryocut with a diamond knife at ca. −120°C and used without staining.

To get a deeper insight into the possible interaction between LS and rubber, Fourier transform infrared spectroscopic (FTIR) measurements were also done. FTIR on the films was performed in the attenuated total reflection mode (ATR) at a resolution of 4 cm^{-1} by using a Nicolet P510 spectrometer (Madison, WI, USA). LS powder was pressed with KBr powder for FTIR measurements in the transmission mode.

Property assessment

Dynamic mechanical thermal analytic (DMTA) spectra of the films were recorded by an Eplexor 25N device (Gabo Qualimeter, Ahlden, Germany) in tension mode at 10 Hz frequency. The complex elastic modulus, its constituents (viz. storage, E', and loss parts, E''), along with the mechanical loss factor (tan δ), were determined as a function of the temperature (T = −100°C . . . +60°C). The static and dynamic tensile loads applied were 2 and $\pm 1N$, respectively, and the heating rate was set to 2°C/min.

Tensile tests, to determine the ultimate properties (strength, elongation), along with the moduli at selected elongations were performed at room temperature (RT) on dumbbells according to ASTM D412 by using a 500 mm/min crosshead speed. The tear strength at RT was determined according to ASTM D624 by using crescent-shaped specimens at a crosshead speed of 500 mm/min. The tensile and tear properties were determined also after heat aging (storage for 7 days at 70°C).

RESULTS AND DISCUSSION

Morphology

Figure 1 shows the XRD spectra of the LS and the LS-containing films of various compositions. Note that the LS shows two smaller peaks in addition to the major peak. These peaks correspond to the following interlayer distances based on the Bragg's equation: 1.22, 1.10, and 0.95 nm; so, the LS used contained some small fractions with higher intergallery distance than the bulk material. LS has been intercalated by NR in the related compound as the interlayer distance of the LS increased to 1.19–1.31 nm. The appearance of the related broad peak suggests that the degree of NR intercalation is different. Considerably better intercalation was noticed for the PUR latex where two peaks

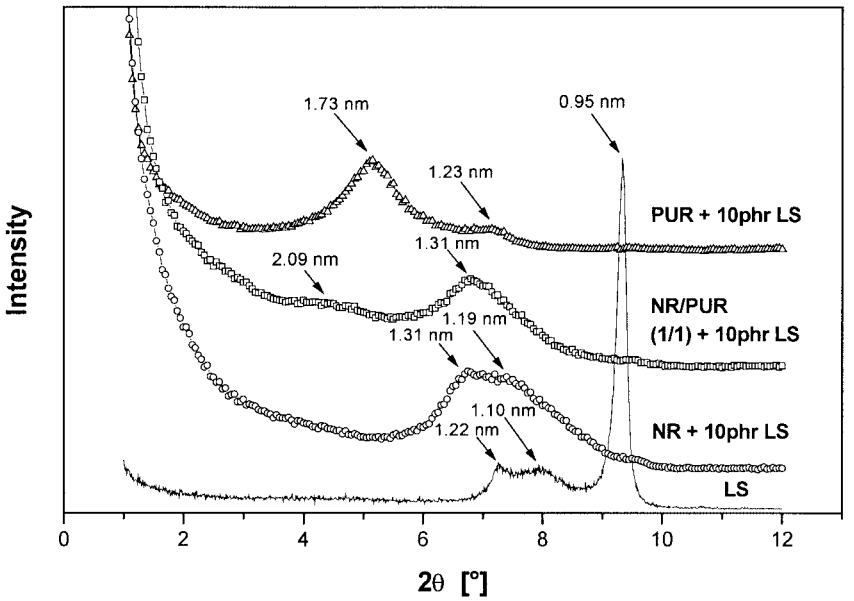

Figure 1 XRD spectra of the layered silicate (LS) reinforced latex nanocomposites of various compositions. [Note. For comparison purposes, this figure contains the XRD spectrum of the LS (sodium fluorohectorite) as well.]

were resolved. The major peak indicates that the interlayer distance of the LS widened to 1.73 nm from the initial 0.95 nm. This effect can be assigned to the higher polarity of PUR compared to NR, which favors the compatibility with LS. Similar to PUR, the NR/PUR latex blend also shows two peaks. Albeit they appear at slightly higher interlayer distances than in PUR, these peaks are the same. The intensity ratio of these peaks is, however, opposed to that of the pure PUR nanocomposite. Before discussing this aspect, attention should be paid to results achieved by TEM and FTIR.

TEM pictures in Figure 2 evidence the good intercalation of LS by PUR. One may get the impression that a part of LS has even been exfoliated. Pictures in Figure 2 demonstrate further the high-aspect ratio of the LS. This becomes more obvious when the size of the flat-laying platelets (disks) in Figure 2(b) is considered.

The dispersion of LS in PUR/NR (1/1) latex blend differs considerably from that of the PUR. The TEM picture in Figure 3 shows that NR and PUR are not compatible. Note that particles from the sulfur prevulcanized NR appear dark in these TEM images. Layered silicate stacks can be located at the boundary of the PUR (light) and NR (dark) phases. Pronounced intercalation and possible exfoliation took place only in the PUR phase [see Fig. 3(b)]. The silicate layers and aggregates cover the NR particles, resulting in a skeleton (house of cards) structure. This peculiar morphology is rather specific for NR nanocomposites produced by the latex route if the length of the LS is commensurable with that of the rubber particle size in the latex. Based on the TEM results, we can now explain the difference in the XRD spectra of the PUR and PUR/NR latices. Recall that LS is less intercalated by NR than by PUR. So, in the case of the PUR/NR blend, PUR should intercalate double the amount of LS because the volume is excluded by NR. Bearing in mind that there is an optimum in the LS content in respect to intercalation/exfoliation phenomena, a substantial increase in the LS may cause its reaggregation (confinement). However, this does not necessarily yield a deterioration in the mechanical properties. Recall that the prevulcanized NR particles force the silicate aggregates in the neighboring PUR phase to cover their surface. This results in a skeleton morphology as the length of the silicate layers is higher than those of the diameter of the particles (Fig. 3). The formation of this skeleton structure may yield improved mechanical properties.

Interesting information can be derived from the FTIR analysis, too. Several attempts to characterize PUR/clay[12–14] or NR/clay[15–16] nanocomposites by using FTIR spectroscopy have already been made. In most of the cases, just verification of the incorporation of the clay into the matrix was the outcome. Differences between the spectra of unfilled material and nanocomposite were sought among peaks corresponding to vibrations of the macromolecular chains of either PUR or NR. Chen et al.[12] tried to estimate the degree of interaction between the silicate layers and the PUR segments evaluating the ratio of the absorption peaks of the hydrogen-bonded and the free groups of NH or C═O. Creation of hydrogen bonds between functional groups of the polymer matrix and

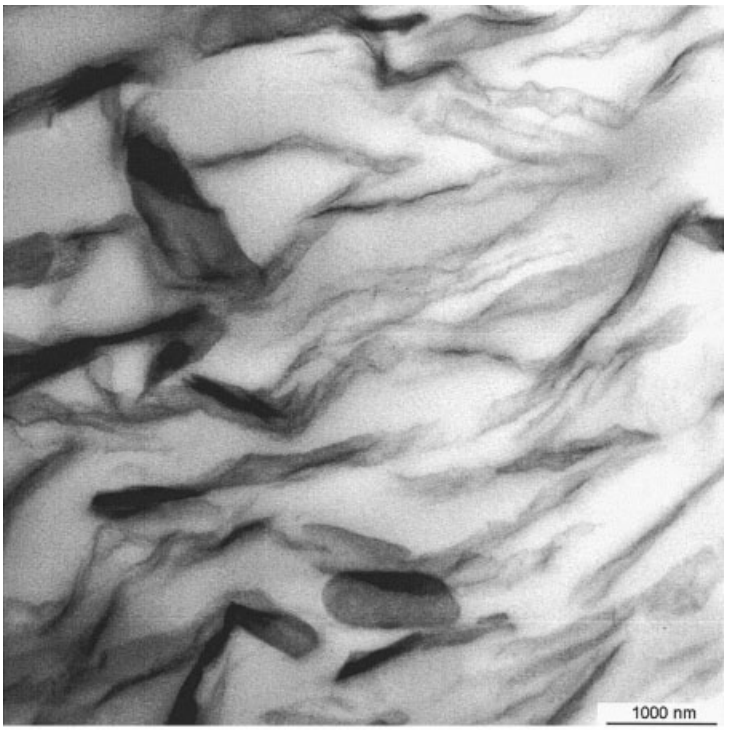

(a)

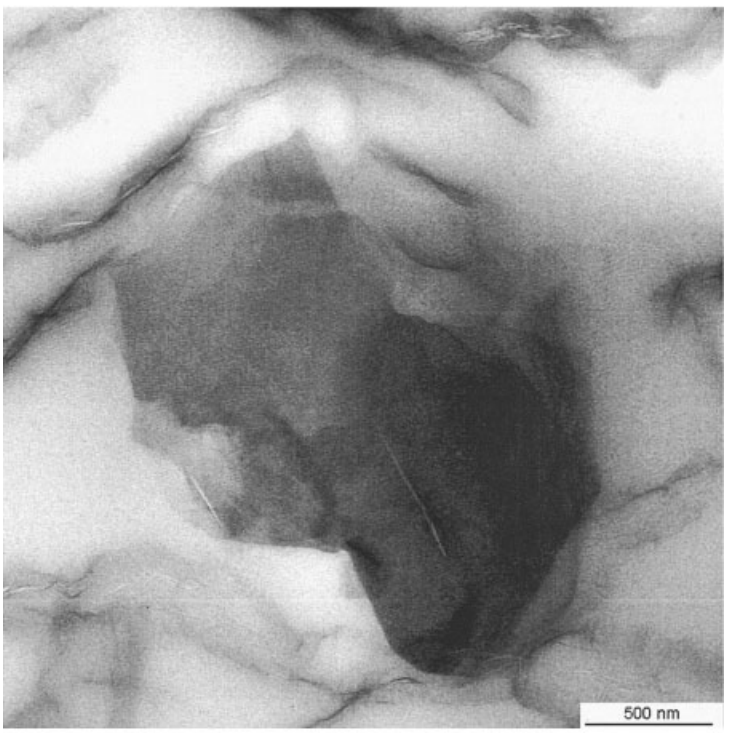

(b)

Figure 2 TEM images taken at various magnifications from the film cast of PUR latex containing 10 phr LS.

the organoclay as well as their maintenance on increasing temperature was examined by Lee and Han for polycarbonate[17] and polystyrene-*block*-hydroxylated polyisoprene copolymer.[18] Recently, Loo et al.[19] monitored the stress-induced peak shift in the Si—O stretching vibration of montmorillonite clay in nylon-6/nanoclay nanocomposite. The vibration of the Si—O bond was found to be sensitive to stress, show-

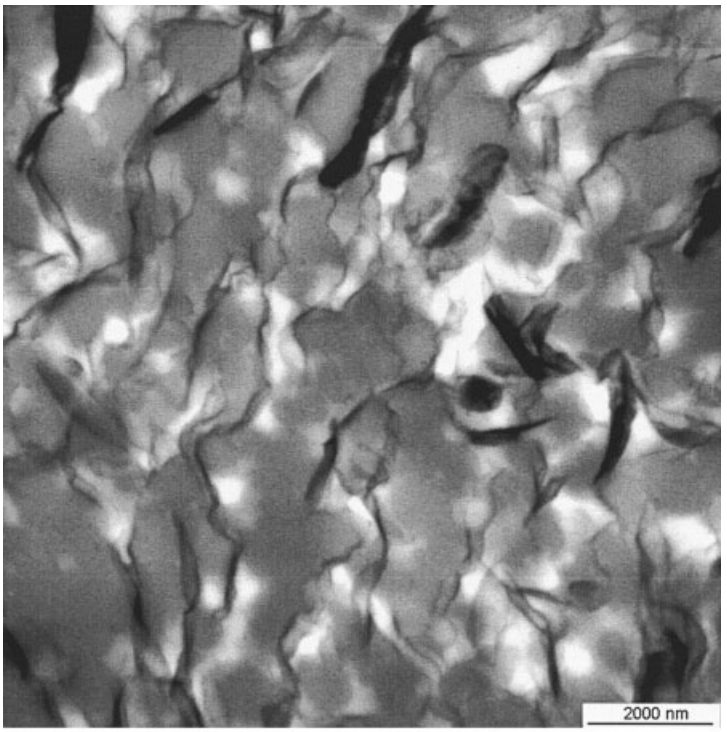

(a)

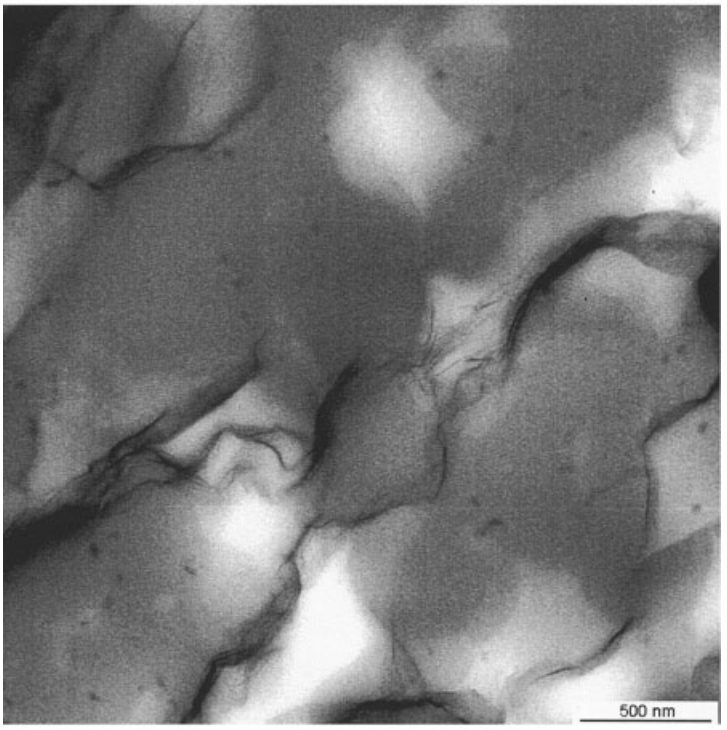

(b)

Figure 3 TEM pictures taken from the film cast of the PUR/NR (1/1) latex blend containing 10 phr LS.

ing a shift to lower wavenumbers with increasing level of strain.

The absorption bands in the infrared (IR) spectrum of various layered silicates depend on their chemical composition.[20] In the case of fluorohectorite, the IR spectrum presents mainly two peaks corresponding to the Si—O stretching vibration, ν (Si—O), at the 1005 cm^{-1}, and the Si—O bending vibration, δ (Si—O), at

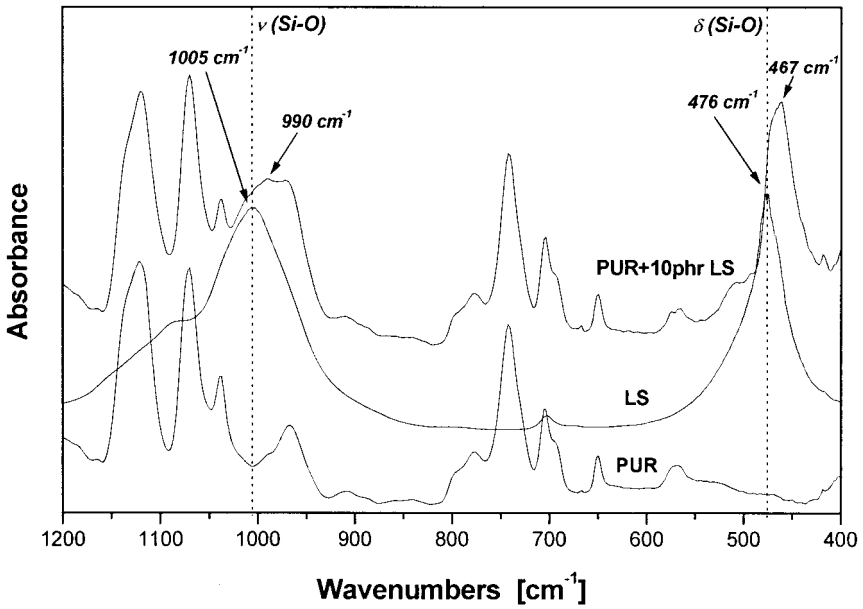

Figure 4 FTIR spectra of PUR, LS, and PUR reinforced with LS 10 phr.

476 cm^{-1}.[13,19,20] The sensitivity of these peaks to intercalation/exfoliation phenomena was observed in the current article.

As presented in Figure 4, the Si—O stretching vibration, at 1005 cm^{-1} in the case of the PUR/LS system, appears as a shoulder around 990 cm^{-1} superposed on the 967 cm^{-1} peak of PUR. Moreover, the Si—O bending vibration at 476 cm^{-1} is shifted to 467 cm^{-1}, presenting a clear peak due to the fact that at that region the PUR does not show any peak. Considering the fact that the PUR is capable of intercalating the layers of LS (i.e., TEM and WAXS experiment), the peak position is likely to be due to the interaction of the macromolecular chain with the silicate layers.

Figure 5 presents the spectra in the case of the NR/LS system. The Si—O stretching vibration, at 1005 cm^{-1}, and the Si—O bending vibration, at 476 cm^{-1}, are shifted to 998 and 470 cm^{-1}, respectively. According to the TEM and WAXS findings, the NR/LS system showed less significant intercalation (and thus layer expansion) than PUR. This means that the interaction between the NR macromolecular chains and the

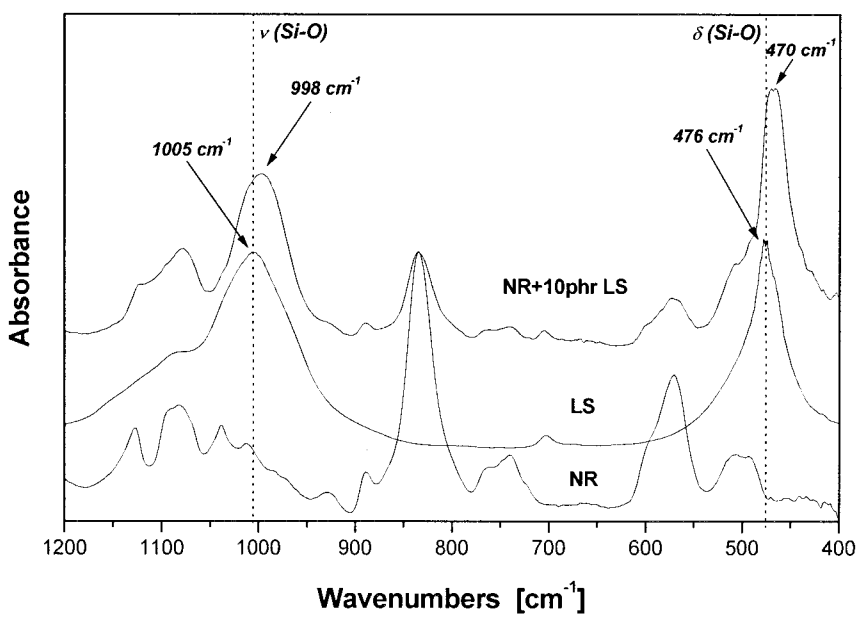

Figure 5 FTIR spectra of NR, LS, and NR reinforced with LS 10 phr.

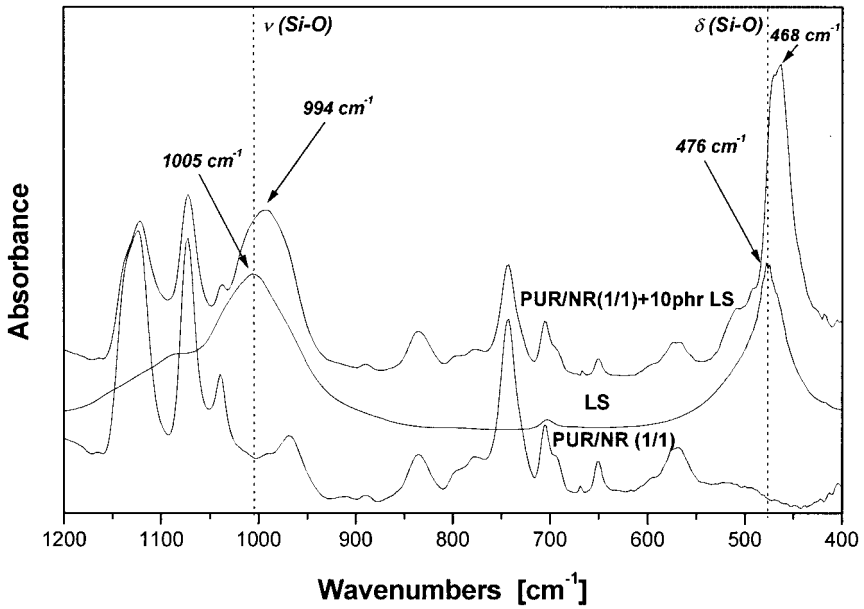

Figure 6 FTIR spectra of PUR/NR (1/1) blend, LS, and PUR/NR (1/1) blend reinforced with LS 10 phr.

layered silicate is rather low. Respectively, the peak shift in the IR spectra for the NR/clay nanocomposite was also smaller than the shift for PUR/clay nanocomposite.

The spectrum of the PUR/NR blend reinforced with LS is presented in Figure 6. The Si—O stretching vibration, at 1005 cm^{-1}, and the Si—O bending vibration, at 476 cm^{-1}, are shifted to 994 and 468 cm^{-1}, respectively. This means that there is a rather good intercalation of LS in the blend, similar to the neat PUR. Considering the TEM images, the component that worked as an intercalant in the blend was the PUR rather than the NR.

Consulting the above-mentioned results, it is clear that PUR has two favorable peaks in the case of the XRD spectra. This means that there are two favorable and possible distances between the layers of the silicate during intercalation. In the case of the spectra taken from the blend, these two peaks also appear but with totally opposite intensity. The volume during drying the latex compound (glass plates) was the same each time and LS is obviously better intercalated by PUR than by NR (XRD spectra). Considering the fact that, in the blend, the volume of the better intercalating PUR is one-half, some excluded volume phenomena may appear, eventually causing restricted mobility of the macromolecular chains. The LS is mainly in the PUR area (TEM images), so the amount of LS that should be intercalated by PUR is not actually 10 phr but almost double. Having in mind that there is an optimum in LS content for intercalation/exfoliation processes,[1,21–22] the increase of LS content in the PUR should have an adverse effect (i.e., intercalation/exfoliation to a lesser extent). This is reflected by the positions and ratio of the XRD peaks in Figure 1 for the NR/PUR blend based composite.

Thermomechanical properties

Figure 7 shows the trend of the storage modulus [E', Fig. 7(a)] and mechanical loss factor [tan δ, Fig. 7(b)] as a function of temperature for the latices studied. Comparing the DMTA traces of the plain rubbers with that of the blend, one can notice that PUR and NR are fully incompatible. This is based on the fact that no change in the related glass transition temperatures (T_g) occurs due to blending and the stiffness response follows the composition ratio. This finding is in harmony with the TEM results. The nano-reinforcement proved to be very efficient below the T_g of the matrix (plain rubbers) and below the component with the higher T_g (blend rubbers), respectively. The stiffness of the plain rubbers was increased by 1200–1500 MPa (depending on the temperature) owing to 10% LS. One can notice that the formation of a skeleton structure in NR and PUR/NR blend is as efficient as the markedly better intercalation, however, without skeleton structure in PUR [cf. Figs. 2(a) and 3(a)]. Figure 7(b) demonstrates that nano-reinforcement caused a dramatic decrease in the tan δ. This finding is in agreement with the expectation: the molecular mobility is strongly hampered owing to the strong LS/rubber interactions. Note that in Figure 7(a) the major consequence of blending NR with PUR is obvious: the blend exhibits a markedly higher stiffness than NR up to $T \approx 10°C$ (T_g of PUR).

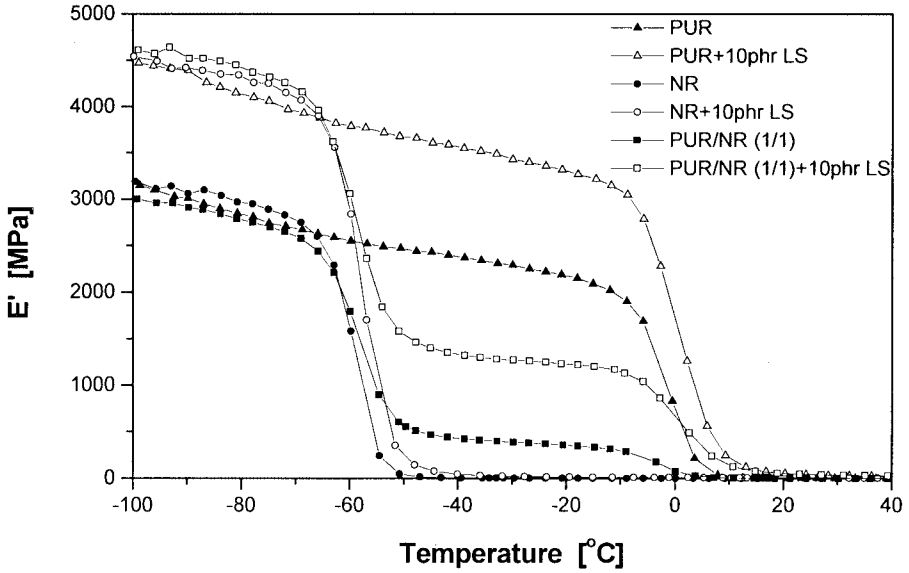

(a)

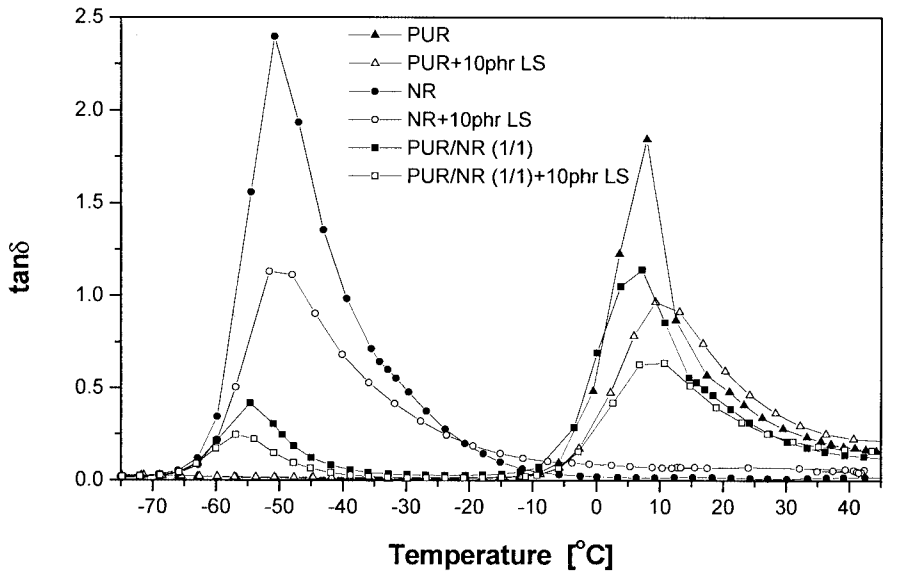

(b)

Figure 7 Storage modulus and mechanical loss factor as a function of temperature for pure and reinforced systems.

Tensile mechanical properties

Table II lists the mechanical properties of the rubbers and their nanocomposites before and after heat aging. Note that LS nano-reinforcement was very effective for PUR. The ultimate tensile strength as well as tear strength were strongly increased (more than three times) and a dramatic improvement was found in the moduli at different elongations. As expected, the LS reinforcement reduced the ultimate elongation. A similar scenario, however, with less improvement in the stiffness and strength, was found for the NR. The most interesting results, for the PUR/NR (composition ratio: 1/1 and 8/2) blend-based nanocomposites, were due to their excellent mechanical performance. So, part of the expensive PUR latex can be replaced by inexpensive NR latex without sacrificing the mechanical response of the nanocomposites. A further consequence of compounding NR with PUR is related to the aging of the latter. Heat aging of PUR accompanied by crosslinking (via interchange reactions), which enhanced the stiffness and strength data of PUR, PUR-containing blend, and related nanocomposites.

CONCLUSION

On the basis of this work, devoted to a study of the morphology-dependent mechanical properties of LS

TABLE II
Mechanical Properties of the Rubber Nanocomposites Studied

Property	PUR	PUR + LS 10 phr	NR	NR + LS 10 phr	PUR/NR (1/1) + LS 10 phr	PUR/NR (8/2) + LS 10 phr
			Before aging			
Tensile strength (MPa)	4.0	15.9	19.6	23.5	12.4	11.4
Tensile modulus (MPa)						
100% Elong.	0.8	5.6	0.7	2.1	4.3	4.9
200% Elong.	0.9	7.8	0.9	3.1	5.9	6.7
300% Elong.	1.1	10.1	1.1	4.5	7.5	8.4
Elongation at break (%)	932	543	881	697	556	469
Tear strength (kN/m)	12.3	54.5	28.0	36.7	59.9	50.7
			After aging at 70°C for 7 days			
Tensile strength (MPa)	10.5	17.9	20.8	23.5	16.7	17.5
Tensile modulus (MPa)						
100% Elong.	1.1	7.6	0.7	2.7	6.7	7.4
200% Elong.	1.4	10.7	0.9	4.2	9.4	10.4
300% Elong.	1.8	13.5	1.1	6.0	11.6	13.0
Elongation at break (%)	772	444	768	620	484	447

reinforced NR-, PUR-, and PUR/NR-blend based nanocomposites produced by the latex route, the following conclusions can be drawn.

LS is more compatible and thus better intercalated by PUR than by NR. In the case of sulfur-prevulcanized NR latex, and its blends with PUR, the LS forms a skeleton (house of cards) structure. The onset of this structure is favored by the prevulcanization of the NR. The reinforcing efficiency of the skeleton-type structure (NR) was comparable with that composed of LS layers and stacks (PUR).

Albeit that PUR and NR are completely incompatible, the mechanical properties of the nanocomposites based on their blends (PUR/NR ratios 1/1 and 8/2) agreed with those of the plain PUR. The effect of LS dispersion (intercalation/exfoliation) was best reflected in stiffness- and strength-related characteristics.

Dr. S. Varghese, K. G. Gatos, and Dr. A. A. Apostolov acknowledge the support of the Alexander von Humbolt Foundation, German Science Foundation (DFG-GRK 814), and German Academic Exchange (DAAD), respectively.

References

1. Karger-Kocsis, J.; Wu, C.-M. Polym Eng Sci to appear.
2. Utracki, L. A.; Kamal, M. R. Arab J Sci Eng 2002, 27, 43.
3. Pinnavaia, T. J.; Beall, G. W., Eds. Polymer–Clay Nanocomposites; Wiley: New York, 2000.
4. Varghese, S.; Karger-Kocsis, J. Polymer 2003, 44, 4921.
5. Zhang, L.; Wang, Y.; Wang, Y.; Sui, Y.; Yu, D. J Appl Polym Sci 2000, 78, 1873.
6. Wang, Y.; Zhang, L.; Tang, C.; Yu, D. J Appl Polym Sci 2000, 78, 1879.
7. Wu, Y.-P.; Jia, Q.-X.; Yu, D.-S.; Zhang, L.-Q. J Appl Polym Sci 2003, 89, 3855.
8. Wu, Y.-P.; Zhang, L.-Q.; Wang, Y.-Q.; Liang, Y.; Yu, D.-S. J Appl Polym Sci 2001, 82, 2842.
9. Cai, H.-H.; Li, S.-D.; Tian, G.-R.; Wang, H.-B.; Wang, J.-H. J Appl Polym Sci 2002, 87, 982.
10. Stephen, R.; Raju, K. V. S. N.; Nair, S. V.; Varghese, S.; Oommen, Z.; Thomas, S. J. Appl Polym Sci 2003, 88, 2639.
11. Varghese, S.; Karger-Kocsis, J.; Gatos, K. G. Polymer 2003, 44, 3977.
12. Chen, T. K.; Tien, Y.-I.; Wei, K.-H. Polymer 2000, 41, 1345.
13. Zhang, X.; Xu, R.; Wu, Z.; Zhou, C. Polym Int 2003, 52, 790.
14. Tien, Y. I.; Wei, K.-H. Polymer 2001, 42, 3213.
15. Joly, S.; Garnaud, G.; Ollitrault, R.; Bokobza, L.; Mark, J. E. Chem Mater 2002, 14, 4202.
16. Arroyo, M.; López-Manchado, M. A.; Herrero, B. Polymer 2003, 44, 2447.
17. Lee, K. M.; Han, C. D. Polymer 2003, 44, 4573.
18. Lee, K. M.; Han, C. D. Macromolecules 2003, 36, 804.
19. Loo, L. S.; Gleason, K. K. Macromolecules 2003, 36, 2587.
20. Mookherjee, M.; Redfern, S. A. T. Clay Miner 2002, 37, 309.
21. Alexandre, M.; Dubois, P. Mater Sci Eng Reports 2000, 28, 1.
22. Kim, J.-T.; Oh, T.-S.; Lee, D.-H. Polym Int 2003, 52, 1058.